N89 - 25199

INVOLUTE COMPOSITE DESIGN EVALUATION
USING GLOBAL DESIGN SENSITIVITY DERIVATIVES

J. K. Hart and E. L. Stanton

PDA Engineering
Costa Mesa, California

Involute Composite Design Overview

The strong interaction between material architecture, processing and structural performance for nozzle components was described at an earlier NASA symposium for laminated involute composites. Since that meeting the Space Shuttle SRM nozzle has test fired involute nozzle components and progress has been made in analyzing their sensitivity to ply pattern design. The parameters that control ply pattern shape [1,2] also control tooling for the manufacture of involute composite structures. In the current CAD/CAM idiom these parameters might be called material form features and they provide a basis for global composite design sensitivity derivatives. They are not to be confused with laminate point design parameters that ignore ply continuity constraints present in finite dimension structural components with curvature. We first define the involute design problem and illustrate these commonly used approaches for composite shell structures. Then analytic sensitivity derivatives are developed and used to analyze test rings and cones with maximum stress failure criteria.


DESIGN VARIABLES

N — Number of Plies

ϕ_0 — Bias Angle

$r_s(z)$ — Start Line

88-0228
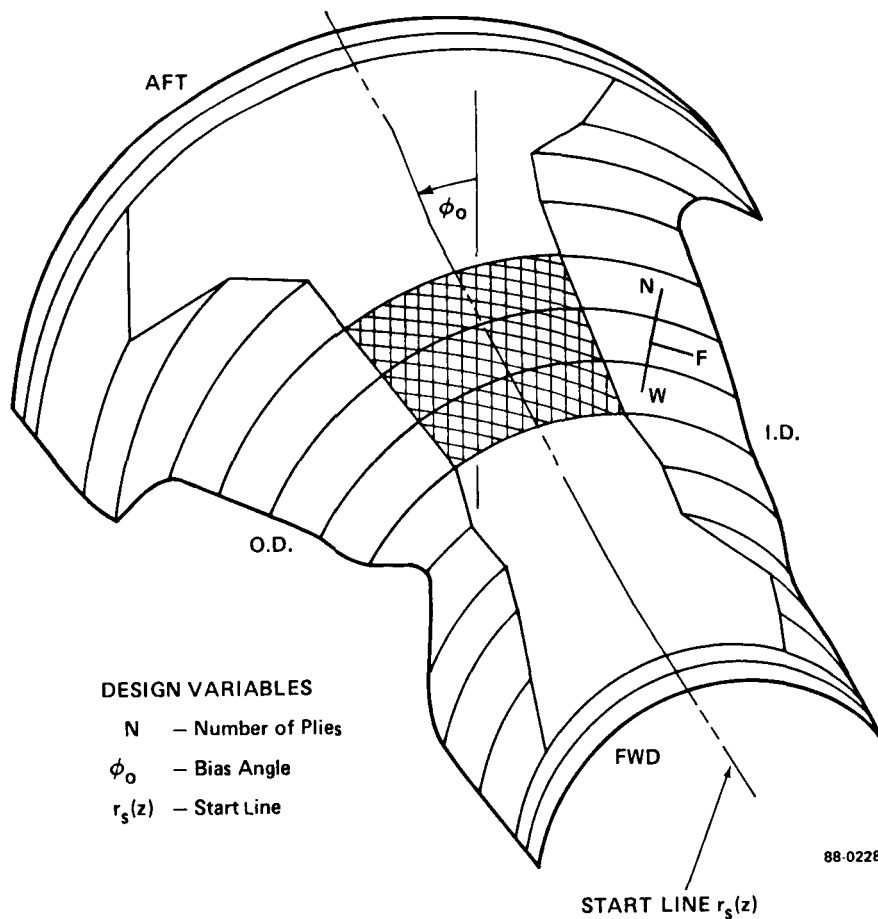
Involute Exit Cone
Ply Material Distribution

The figure below illustrates the orientation of the plies in a conical section of an involute exit cone. The intersection of a ply with a plane defined by a constant Z coordinate (e.g., curves AD and BC) is an involute curve. Each ply can be mapped to an adjacent ply by a rotation of θ degrees about the axis of symmetry, where

$$\theta = \frac{360°}{N}$$

and N is the number of plies in the involute structure.
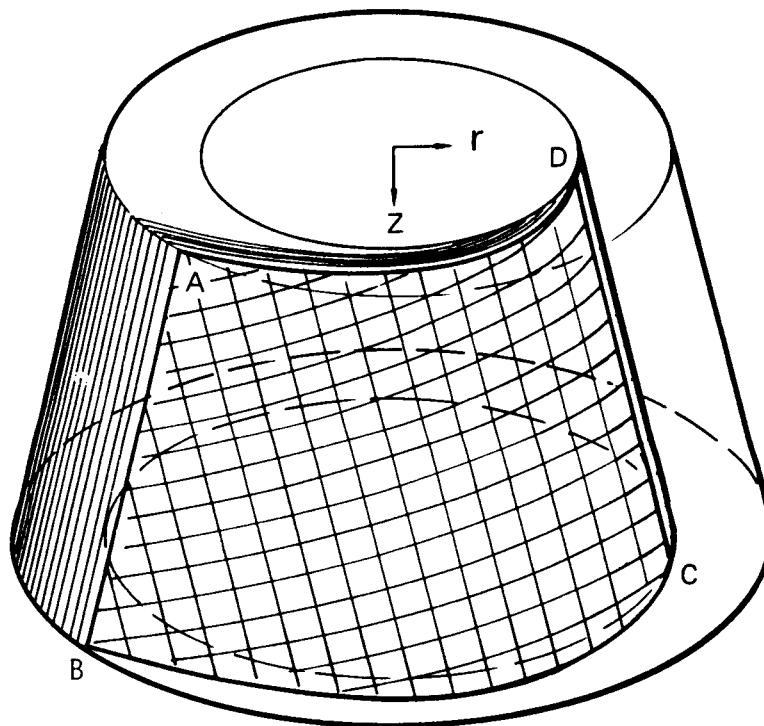
Involute Design Practice

Industrial practice in the U.S. for involute ply pattern design at one time was limited to either ID or OD start lines partly because of the geometric complexity of the problem. Both of these design approaches have one straight edge which also makes layup and inspection easier. On the negative side these patterns are more difficult to form to shape and do not insure fiber continuity in critical stress regions. An alternative approach used by PDA places the start line near the midsurface of the net part to insure fiber continuity. Typically a great many patterns are examined by trial and error using CAE tools in designing involute composite structures. Low manufacturing risk and high margins of safety during a motor firing are the figures of merit. The shape of the component, hence weight, is prescribed in most cases and rarely is this shape open to significant change. The shape of the ply pattern in contrast is open to wide variations and suggests the need for design sensitivity analyses to improve trial and error procedures and ultimately to automate the procedure.
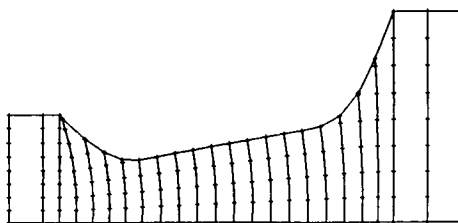
O.D. Start-line Ply Pattern
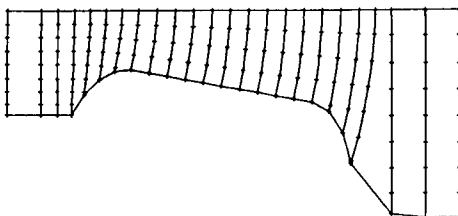
PDA Start-line Ply Pattern
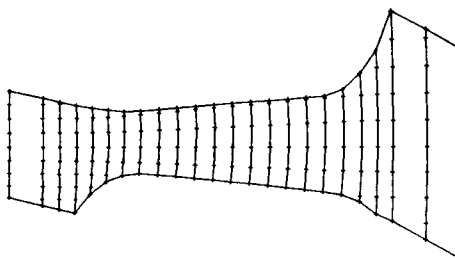
I.D. Start-line Ply Pattern

Involute Design Variables

The design space includes the ply count and the ply thickness product Nt, the helix angle ϕ_0, and up to 6 variables defining the start line, which is a ply meridian lying in the r-z plane. These variables determine at each node three Euler angles α, γ, and ϕ which rotate the reference frame into the material frame. From these angles a strain transformation matrix is calculated and the distribution of these matrices within a finite element is used to calculate the element stiffness matrix. This is a global relation independent of finite element mesh.

DESIGN VARIABLES ~ (X)

$$(X) = (Nt, \phi_0, R_s (Z))$$

DEPENDENT VARIABLES ~ Euler Angles α, γ, ϕ

$$\left. \begin{array}{l} \alpha = \alpha(X) \\ \gamma = \gamma(X) \\ \phi = \phi(X) \end{array} \right\} \rightarrow [D(\alpha, \gamma, \phi)]$$

STIFFNESS MATRIX

$$[K] = \left[\int_v [B]^T [D]^T [C_m][D][B] \, |J| \, dV \right]$$

Design Sensitivity Formulation

The direct method of design sensitivity analysis is used. The governing equation for linear statics (equation 1) is differentiated to obtain equation 2. Equation 3 is obtained by solving equation 2 for {dU/dX}. The remainder of the effort is directed toward evaluating {dU/dX}. The finite element analysis already produces the factored stiffness matrix so it is only necessary to evaluate the part of equation 3 in parentheses. The element stiffness matrix in equation 4 and the element thermal load vector in equation 5 (only the thermal load is sensitive to material geometry orientation) may be differentiated to obtain equation 6. The differentiation is simplified because there is no shape sensitivity: the derivative of the strain-displacement transformation matrix [B] is zero. The new matrices [Q] and [R] are functions of the elasticity matrix [C], the strain transformation matrix [D] and its inverse, and the corresponding derivatives, all given in equations 7 and 8. The integrands in equation 6 are developed in closed form. All sensitivity calculations and all finite element analyses are performed by a test version of the P/COMPOSITE module in PATRAN.

Differentiate

$$[K]\{U\} = \{F\} \tag{1}$$

to obtain

$$\left[\frac{dK}{dX}\right]\{U\} + [K]\left\{\frac{dU}{dX}\right\} = \left\{\frac{dF}{dX}\right\} \tag{2}$$

Then

$$\left\{\frac{dU}{dX}\right\} = [K]^{-1}\left(\left\{\frac{dF}{dX}\right\} - \left[\frac{dK}{dX}\right]\{U\}\right) \tag{3}$$

Given

$$[K] = \int_v [B]^T[C][B]\,|J|\,dV \tag{4}$$

and

$$\{F\} = \int_v [B]^T[C]\{\alpha\}\Delta T\,|J|\,dV \tag{5}$$

then

$$\left\{\frac{dF}{dX}\right\} - \left[\frac{dK}{dX}\right]\{U\} = \int_v [B]^T([Q] + [R]^T + [R])\,\{\epsilon_\theta\}\,|J|\,dV$$

$$- \left[\int_v [B]^T([R]^T + [R])\,[B]\,|J|\,dV\right]\{U\} \tag{6}$$

where

$$[Q] = [C]\frac{d}{dX}([D]^{-1})[D] \tag{7}$$

and

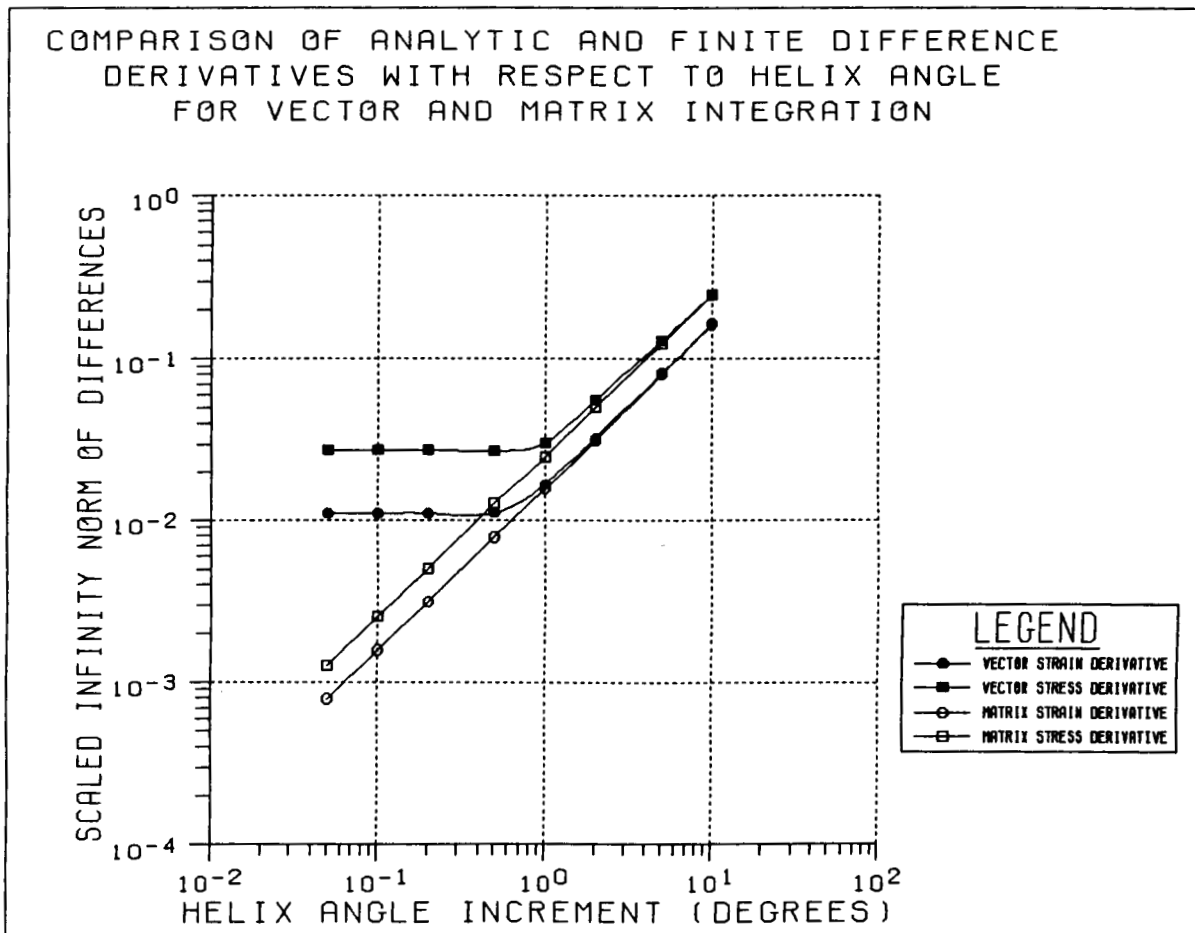$$[R] = [C][D]^{-1}\frac{d}{dX}([D]) \tag{8}$$

Vector and Matrix Sensitivity Integration

Originally the sensitivity integration (equation 6) was performed by inserting the $\{U\}$ vector inside the second integral and making the substitution

$$\{\varepsilon\} = [B]\{U\}$$

to convert the matrix integration to a vector integration. The economy of this approach is evident, but finite difference tests show a failure to converge manifested by a "plateau" phenomenon for step sizes below a certain threshold. The onset of this deviation occurs at a step size that is too large to be attributable to round-off error. Because of this error, it was decided that matrix integration would be used for all sensitivity calculations.

The accompanying graph was generated for the helix angle design variable in a 439 degree of freedom test cone problem, and the error shown is typical.

COMPARISON OF ANALYTIC AND FINITE DIFFERENCE DERIVATIVES WITH RESPECT TO HELIX ANGLE FOR VECTOR AND MATRIX INTEGRATION

LEGEND
— ● — VECTOR STRAIN DERIVATIVE
— ■ — VECTOR STRESS DERIVATIVE
— ○ — MATRIX STRAIN DERIVATIVE
— ▱ — MATRIX STRESS DERIVATIVE

Formulation of Optimization Problem

The objective of the optimization is to minimize risk. To this end, the shape (and thus the weight) of the part are fixed and the optimization is used to find the ply pattern design furthest from the constraint surfaces, subject to manufacturing and side constraints. The mathematical formulation of the optimization problem is given below. The objective function is a slack variable β which represents the load margin (i.e., the distance between the load index and unity) to be maximized. The slack variable is added to each response constraint g_j. In addition, there are manufacturing constraints h_k which do not require the buffer of the slack variable. The Method of Feasible Directions algorithm [3] in MICRODOT is used to solve the primal form of the optimization problem. Dual methods are not used because the number of constraints is much greater than the number of design variables. Approximation concepts [4, 5, and 6] are used to formulate the sequence of approximate problems.

$$\beta \to \max$$

Subject to

$$g_j(X) + \beta \leq 0 \qquad j = 1,2,...,m$$

$$h_k(X) \leq 0 \qquad k = 1,2,...,\ell$$

$$X_i^\ell \leq X_i \leq X_i^u \qquad i = 1,2,...,n$$

Manufacturing Constraints on Design Parameters

Two of the manufacturing constraints alluded to on the previous page are shown in the picture below. The central angle is the angle subtended by a ply as it extends from the inner radius to the outer radius, and the arc angle is the angle between a ply surface tangent and the circumferential direction. Good design practice for nozzle components dictates that the central angle should not exceed 120 degrees and the arc angle should not exceed 10-15 degrees.
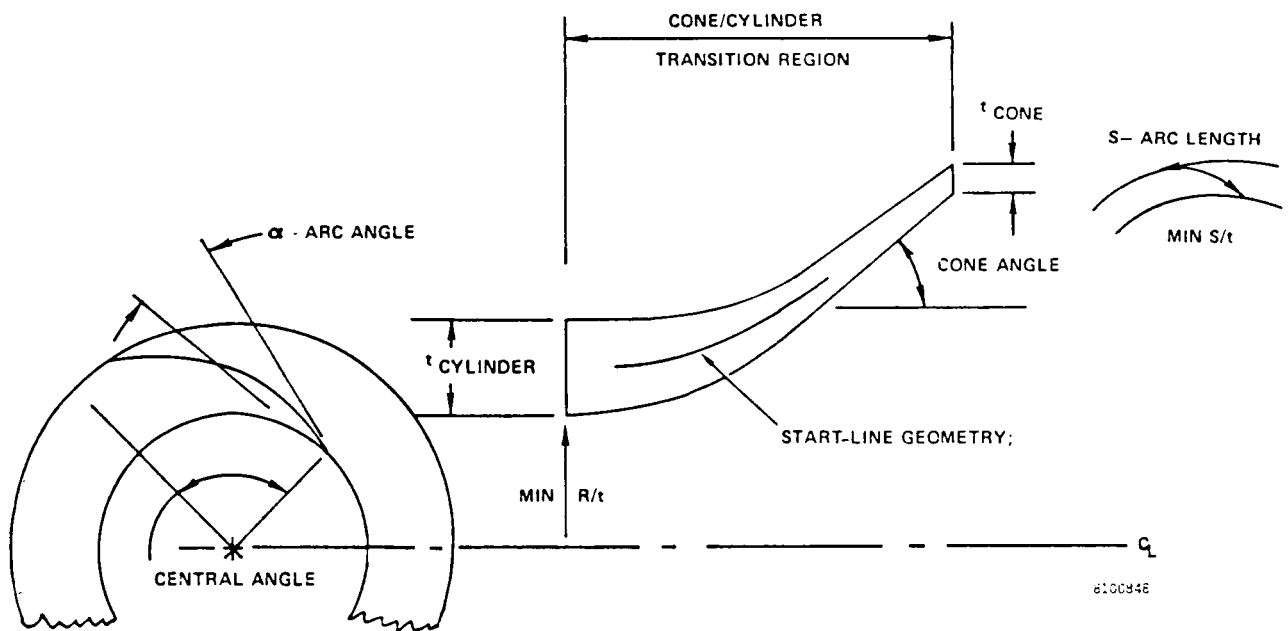
First Optimization Sequence For Involute Ring Problem

The first optimization problem is an axisymmetric carbon-carbon cylinder having 82 degrees of freedom. The design variables are the helix angle ϕ and the slope m. Five iterations are required to increase the margin of safety from .708 at the starting point to 1.055 at the optimum.

FIRST OPTIMIZATION PATH FOR INVOLUTE RING
INTERNAL PRESSURE LOAD. MAX STRESS CRITERION
MARGIN OF SAFETY SHOWN FOR EACH ITERATION
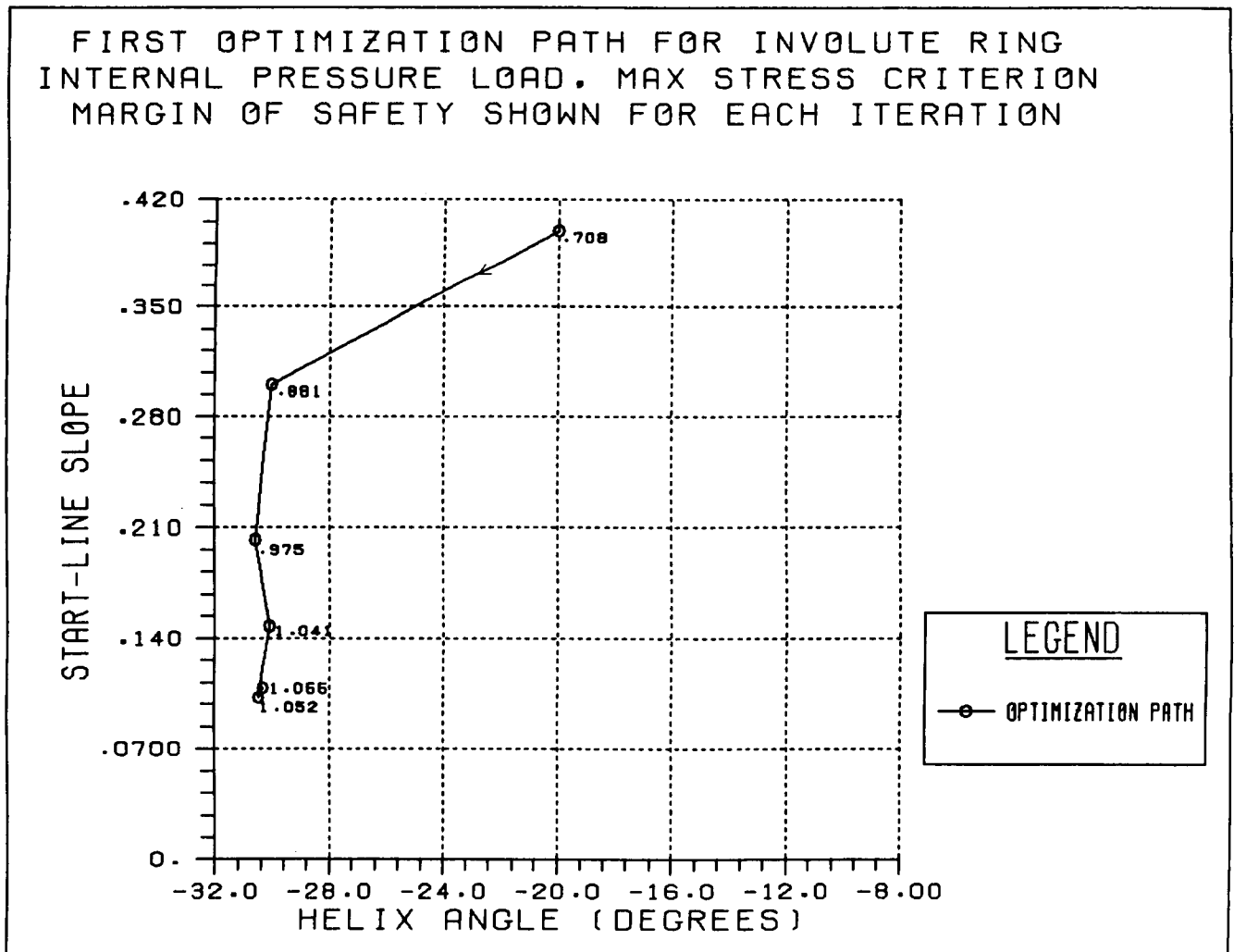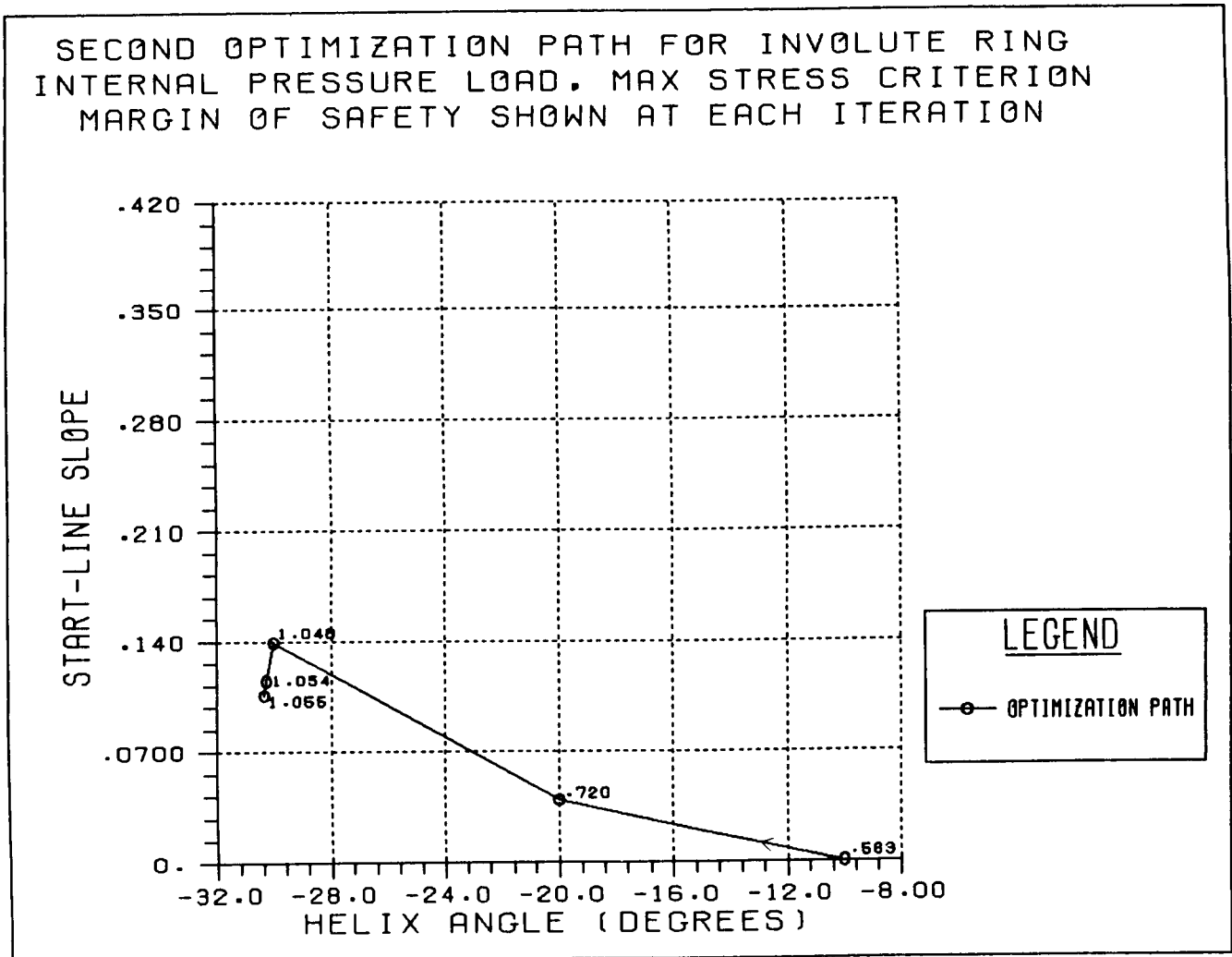
Summary Table for First Optimization Path

The iteration history of the first optimization path is shown in Table 1. In the course of the optimization the critical stress component varies from fill tension in the outer element at the beginning to in-plane shear on the inner radius at the optimum. As the optimization proceeds, the constraint tolerance is reduced from .03 to the value of .001 required for convergence. The finite difference tests on the sensitivity derivatives were used to select move limits that would predict the response to within about 10 percent. The optimization results indicate that this choice was conservative enough.

TABLE 1

Objective Function	Margin of Safety	Design Variables ϕ_0	Design Variables m	Move Limits $\Delta\phi_0$	Move Limits Δm	Constraint Tolerance	Most Critical Constraint Node	Most Critical Constraint Component	Number of Active Constraints	Number of Gradient Evaluations	Number of Function Evaluations
.4144	.7077	-20.000°	.4000				13	T2			
.4682	.8806	-30.000°	.3000	10°	.1	.03	25	T2	3	3	15
.4938	.9755	-30.556°	.2022	10°	.1	.03	4	S12	9	2	31
.5100	1.0409	-30.071°	.1478	10°	.1	.008	3	S12	15	2	5
.5127	1.0522	-30.440°	.1019	10°	.1	.008	3	S12	9	3	4
.5133	1.0547	-30.297°	.1086	10°	.1	.001	3	S12	3	2	2

Second Optimization Sequence For Involute Ring Problem

A different starting point is used for the same optimization problem. Here four iterations are required to increase the margin of safety from .563 at the starting point to 1.055 at the optimum. Note that the same optimum is reached in both cases.

SECOND OPTIMIZATION PATH FOR INVOLUTE RING
INTERNAL PRESSURE LOAD. MAX STRESS CRITERION
MARGIN OF SAFETY SHOWN AT EACH ITERATION

Summary Table for Second Optimization Path

The iteration history of the second optimization path is shown in Table 2. Although the margin of safety shows greater improvement along this path, fewer iterations are required. Throughout the optimization the critical region is along the inner radius. The critical stress component varies from fill tension at the beginning to in-plane shear at the optimum. As before, the constraint tolerance is reduced from .03 to the value of .001 required for convergence. Again, the move limits appear conservative enough.

TABLE 2

Objective Function	Margin of Safety	Design Variables ϕ_0	m	Move Limits $\Delta\phi_0$	Δm	Constraint Tolerance	Most Critical Constraint Node	Component	Number of Active Constraints	Number of Gradient Evaluations	Number of Function Evaluations
.3602	.5629	-10.000°	0.0000				2	T2			
.4184	.7195	-20.000°	.0390	10°	.1	.03	2	T2	4	2	29
.5118	1.0482	-30.000°	.1390	10°	.1	.03	1	T2	4	3	27
.5131	1.0537	-30.247°	.1144	10°	.1	.001	3	S12	3	2	5
.5134	1.0551	-30.324°	.1057	10°	.1	.001	3	S12	3	2	2

Involute Test Cone Optimization

The second optimization problem is an axisymmetric carbon-carbon test cone tested and analyzed by Stanton and Kipp [7] and having 439 degrees of freedom. The model is subjected to an axial load along the aft rim and is constrained axially along the forward rim. The design variables are the product of the ply count and the ply thickness Nt, the helix angle ϕ_0, and four additional variables controlling the start line. The initial design is the same as the final design selected by Stanton and Kipp: it is therefore expected that the initial design is close to optimal. Four iterations are, in fact, required to increase the margin of safety from 2.653 at the starting point to 2.798 at the optimum.
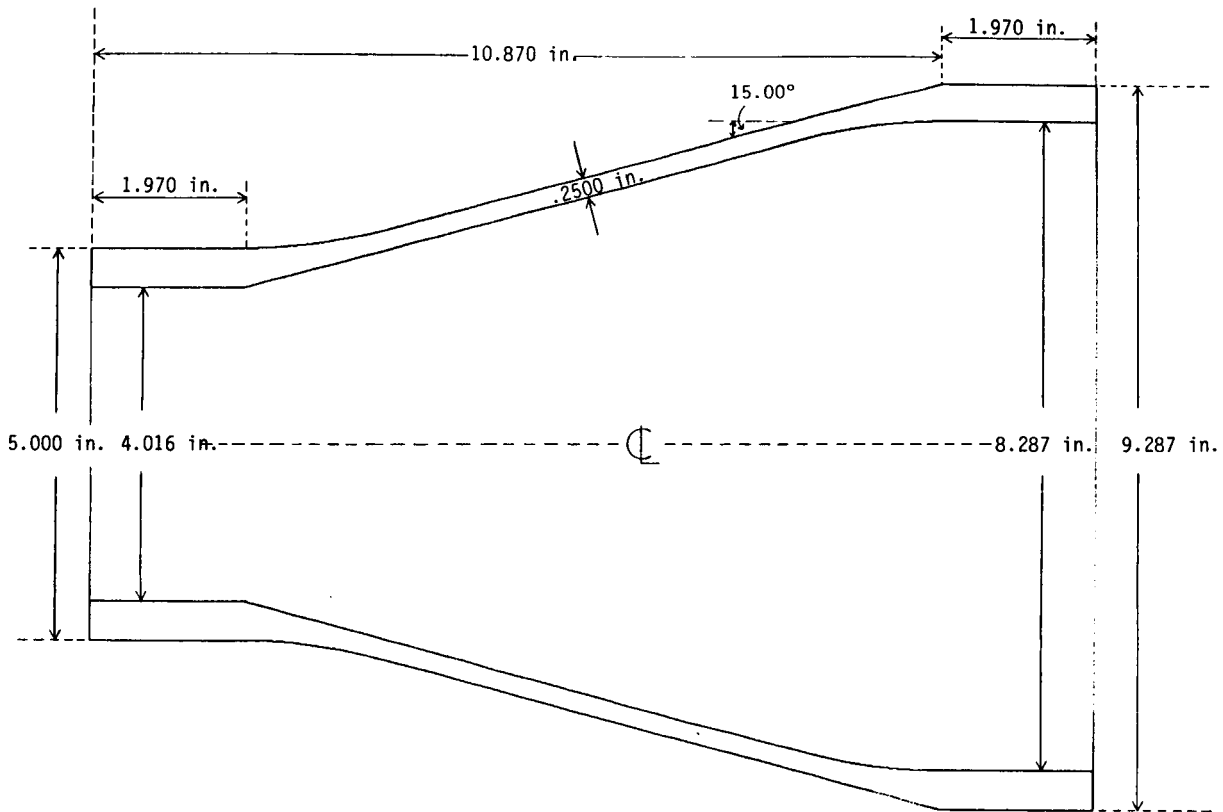
Reference and Optimized Ply Pattern

The reference ply pattern designed by Stanton and Kipp is shown below. The warp aligned test cone design with the start line following the midsurface of the shell was considered radical when it was first discussed with manufacturers. The design goal at that time was to develop the full strength of the carbon-carbon material in the critical cone-cylinder transition under axial load. That too was considered impractical but both are common practice today.

It can be seen that the shape of the optimized ply pattern in the forward region has changed considerably due to changes in the start line. In addition, the width of the ply pattern has been uniformly reduced due to the increase in the ply count and the ply thickness.

REFERENCE PLY PATTERN
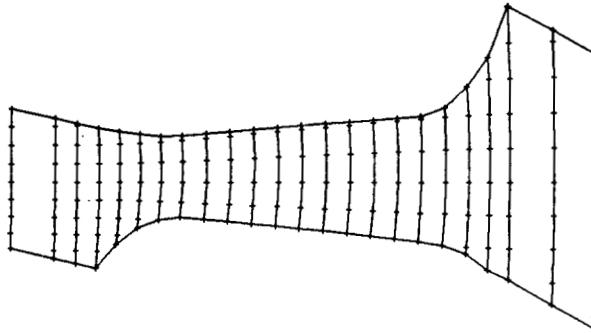
OPTIMIZED PLY PATTERN
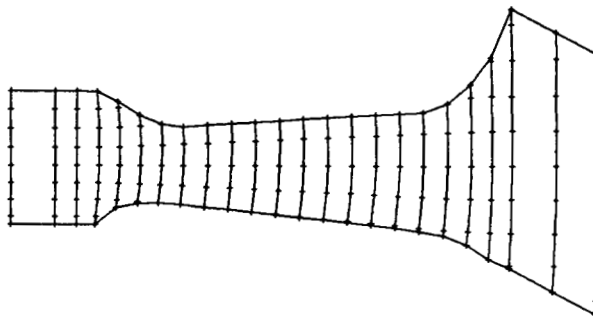
Summary Table For Test Cone Optimization Path

The optimization history for the test cone problem is given below.

(Max Stress Failure Criteria)

Iteration Number	Objective Function	Margin of Safety	Nt	ϕ_0	Y_1	m	Y_2	ξ_2	Node	Component
0	.7263	2.6536	2.2500	0.0000°	2.3200	3.500×10^{-2}	2.6225	.7500	48	C1
1	.7328	2.7418	2.2446	6.0972°	2.3136	7.883×10^{-3}	2.5725	.7640	53	C1
2	.7360	2.7884	2.3803	4.7420°	2.2636	2.217×10^{-3}	2.6225	.7776	48	C1
3	.7366	2.7970	2.3814	5.6872°	2.2389	1.000×10^{-3}	2.6419	.7839	53	C1
4	.7367	2.7983	2.3815	5.6538°	2.2382	1.000×10^{-3}	2.6431	.7841	53	C1

Design Variables; Most Critical Constraint

Iteration Number	ΔNt	$\Delta \phi_0$	ΔY	Δm	ΔY_2	$\Delta \xi_2$	Constraint Tolerance	Number of Active Constraints	Number of Gradient Evaluations	Number of Function Evaluations
0										
1	.4	10°	.05	.05	.05	.2	.001	2	3	14
2	.4	10°	.05	.05	.05	.2	.001	2	4	32
3	.4	10°	.05	.05	.025	.2	.001	3	2	43
4	.4	10°	.05	.05	.025	.2	.0002	3	2	6

Move Limits

Conclusions

An optimization capability for involute structures has been developed. Its key feature is the use of global material geometry variables which are so chosen that all combinations of design variables within a set of lower and upper bounds correspond to manufacturable designs. A further advantage of global variables is that their number does not increase with increasing mesh density. The accuracy of the sensitivity derivatives has been verified both through finite difference tests and through the successful use of the derivatives by an optimizer.

The state of the art in composite design today is still marked by point design algorithms linked together using ad hoc methods not directly related to a manufacturing procedure. The global design sensitivity approach presented here for involutes can be applied to filament wound shells and other composite constructions using material form features peculiar to each construction. The present involute optimization technology is being applied to the Space Shuttle SRM nozzle boot ring redesigns by PDA Engineering.

— A design sensitivity capability using global material geometry variables has been developed.

— The number of global variables is insensitive to finite element mesh density.

— The sensitivity derivatives have been used successfully in an optimization context.

— The sensitivity integral calculations in vector form yielded a tangible error not shared by the corresponding calculations in matrix form.

— The global variable approach can be applied to other composite constructions using material form features peculiar to each construction.

References

1. Savage, E.E., "The Geometry of Involute Construction", JANNAF Rocket Nozzle Technology Subcommittee Meeting 1979, CPIA Publication 310, 1980, pp. 293-308.

2. Pagano, N.J., "General Relations for Exact and Inexact Involute Bodies of Revolution", AFWAL-TR-82-4053, April 1982.

3. Vanderplaats, G.N., "A Robust Feasible Directions Algorithm for Design Synthesis", Proceedings, AIAA/ASME/ASCE/AHS, 24th Structures, Structural Dynamics and Materials Conference, Lake Tahoe, Nevada, May 2-4, 1983.

4. Schmit, L.A. and Farshi, B., "Some Approximation Concepts for Structural Synthesis", AIAA Journal, Vol. 12, No. 5, May 1974, pp. 692-699.

5. Schmit, L.A. and Miura, H., "Approximation Concepts for Efficient Structural Synthesis", NASA CR-2552, March 1976.

6. Lust, R.V. and Schmit, L.A., "Alternative Approximation Concepts for Space Frame Synthesis", NASA CR-172526, March 1985.

7. Stanton, E.L. and Kipp, T.E., "Nonlinear Mechanics of Two-Dimensional Carbon-Carbon Composite Structures and Materials", AIAA Journal, Vol. 23, August 1985, pp. 1278-1284.